Steady-state Modeling of Small Modular Reactors for Multi-timescale Power System Operations with Temporally Coupled Sub-models

Jubeyer Rahman, *Student Member, IEEE,* and Jie Zhang, *Senior Member, IEEE*

***Abstract*—Small modular reactors (SMRs) offer a promising avenue for revolutionizing the traditional role of nuclear plants, transforming them from serving as baseload to flexible contributors in both power generation and ancillary services. This paper develops a steady-state model for SMRs, with a focus on incorporating constraints related to 'xenon poisoning'. 'Xenon poisoning' constraints are integrated into a multi-timescale power system operation framework, which also encompasses inter-temporal coupling constraints. A comprehensive investigation is undertaken to evaluate the impact of integrating SMRs into the NREL-118 bus network. A capacity expansion planning analysis is conducted to identify the optimal locations and sizes for deploying SMRs. To obtain operational details, a production cost model based multi-timescale simulation framework is employed to determine the optimal commitment and dispatch decisions. Additionally, we've developed various reserve rules that adapt to the ramping status of the SMRs. The integration of these physical constraints into the nuclear plant model for multi-timescale steady-state simulation has been achieved while minimizing modeling complexities and computational burdens. Results illustrate that the implementation of minimal 'xenon poisoning' hold-time, coupled with a steady-state guided reserve provision rule, yields the highest revenue – approximately 4.14% more than the base case.**

***Index Terms*—Xenon-poisoning, multi-timescale operation, capacity expansion, flexible operation, small modular reactors.**

NOMENCLATURE

Sets

G	Set of generators
G_{NPP}	Set of nuclear generators
RS	Set of reserve types
T	Set of time slots

Constants

ΔP_g^k	Generation block size of unit g in block k
C_g^k	Generation cost of unit g in block k
H_{DAC}	Number of intervals for DARCUC
H_{RTC}	Number of intervals for RTRCUC
H_{RTD}	Number of intervals for RTRCED
I_{DAC}	Interval length for DAC
I_{RTC}	Interval length for RTC
I_{RTD}	Interval length for RTD
K_g	Block number of generator cost function of unit g
NL_g	No-load cost of unit g
P_g^{max}	Maximum output of unit g
P_g^{min}	Minimum output of unit g
R_g^D	Ramp-down limit for unit g
R_g^U	Ramp-up limit for unit g
RAT_r	Reserve activation time of r type reserve
$RC_{g,r}$	Reserve cost of unit g for type r
RON_r	Whether the unit needs to be 'ON' to provide r type reserve
$RP_{t,r}$	Reserve price at the t^{th} interval for type r
$RRR_{t,r}$	System reserve requirement of type r at time t
SD_g	Shutdown cost of unit g
SU_g	Start-up cost of unit g
$T_{g,t}^{R_{off}^U}$	Ramp-up off enforcement duration of unit g at time t
T_{H_g}	hold-time of unit g
$U_{g,t}^{R_{off}^U}$	Ramp-up off enforcement status of unit g at time t
$VOIR_r$	Cost of insufficient reserve of type r

Continuous Variables

$\overline{p}_{g,t}$	Maximum available power output of unit g at the t^{th} interval
ls_t	Load-shedding penalty at the t^{th} interval
$p_{g,t}$	Power output of unit g at the t^{th} interval
$p_{g,t}^k$	Power output of unit g at the t^{th} interval in block k
$pc_{g,t}$	Production cost of unit g at the t^{th} interval
$rc_{g,t,r}$	Reserve cost of unit g of type r at the t^{th} interval
$rr_{g,t,r}$	Reserve of type r from unit g at the t^{th} interval
$sd_{g,t}$	Shutdown cost of unit g at the t^{th} interval
$su_{g,t}$	Start-up cost of unit g at the t^{th} interval

Integer / Binary Variables

$ramp\_dn_{g,t}$	Ramp-down status of unit g at the t^{th} interval
$ramp\_up_{g,t}$	Ramp-up status of unit g at the t^{th} interval
$stable_{g,t}$	Stable status of unit g at the t^{th} interval
$v_{g,t}$	Commitment status of unit g at the t^{th} interval

I. INTRODUCTION

The role of nuclear power plants is gradually evolving from their traditional 'baseload' operation to a more adaptable 'load-following' or 'ramping' mode, driven by the need for a grid that relies more on renewable energy sources and leaves fewer carbon footprints [1]. Rather than making drastic changes to reactor designs, it's the plant control adjustments

J. Rahman is with the Department of Electrical and Computer Engineering, The University of Texas at Dallas, Richardson, TX 75080, USA.

J. Zhang is with the Department of Mechanical Engineering, and the Department of Electrical and Computer Engineering (Affiliated), The University of Texas at Dallas, Richardson, TX 75080, USA, e-mail: jiezhang@utdallas.edu.

that enable them to respond swiftly to shifting generation mixes and energy prices. Various instances demonstrate the potential for nuclear plants' flexible operation to contribute to the growing need for flexibility in the power system [2] and advocate for policies that incorporate flexibility features in future nuclear plant deployments [3]. As the drive to install more renewable energy sources continues at both the utility and consumer levels, non-flexible resources face challenges in generating sufficient revenue over the long term [1]. Operating in a flexible mode can help nuclear plant owners increase revenue by offering a variety of products, including higher-priced operating reserves when they are in demand. In light of current market dynamics, nuclear plants, regardless of their type, represent a significant capital investment in the energy sector. However, they face increasing challenges in maintaining competitiveness against the backdrop of low-cost natural gas plants and renewable energy sources with minimal operational expenses. The emerging SMR technology, while promising, requires a supportive regulatory framework to foster its expansion. Although SMR technology is advancing and nearing widespread deployment, significant regulatory support, such as tax incentives, is crucial to facilitate its adoption. Yet, it's essential to recognize the multifaceted benefits SMRs offer, including decarbonization, job creation, reliability, and resilience. Many of these advantages transcend monetary evaluation and should be factored into regulatory decision-making processes for a comprehensive assessment of SMR viability.

While small modular reactors have been the subject of extensive research, their large-scale implementation remains an evolving field [4]. In this study, we center our model around a pressurized water reactor (PWR)-based SMR, a prevalent variant in current usage [5]. SMRs possess inherent scalability thanks to their modular design, coupled with advanced safety and flexibility features [6]. This provides them with a distinct advantage in navigating various energy mix scenarios, whether in fossil-dominated power systems or renewable-intensive grids. However, it's important to note that this research does not venture into the complex realm of reactor dynamics. Instead, our focus lies in modeling the steady-state attributes that arise from observed reactor dynamics in various parametric studies.

Control rods are used to adjust the power output of a nuclear plant specially when the plants participate in providing regulation services in flexible operation mode (for example in France and Germany, nuclear plants are used to provide regulation services) [7]–[9]. Their insertion reduces the output and withdrawal increases it. The accuracy of power output control depends on the neutron-absorbing capacity of these control rods. However, rapid control rod maneuvering can lead to significant changes in fuel temperature and, in extreme cases, fuel cladding failure (as seen in the Chernobyl incident where the increased temperature burnt away the 'Xenon' that resulted in a sudden increase in the fission reaction rate leading to the eventual reactor failure [10]). Nuclear plant operators adopt a conservative approach to control rod maneuvering to prevent such incidents, which involves delaying control rod adjustments to ramp up the plant's output following a ramp-down maneuver. This delay period is known as 'hold-time' and typically ranges from 2 to 9 hours, depending on the operational policies of system operators [11]. Even with this conservative plant operation approach, nuclear plant operators can safely manage to operate at a ramp-rate of 2-5.2% of the rated capacity per minute on a regular basis without enhancing the rate of risk of fuel cladding failure [11]. This ramp-rate can reach even higher (upto 10% of the rated capacity per minute in the modern reactors [12]. Fig. 1 illustrates this dispatch scheme of maintaining a delay period, T_H after a ramp-down event to facilitate subsequent ramp-up adjustments. While the qualitative approach in presenting the figure aligns with previous work [11], [13], [14], it does not explicitly depict the underlying mechanisms of 'Xenon-poisoning'. Instead, it illustrates the relationship between the dispatch profile and the unique features of the nuclear plant within the steady-state domain.

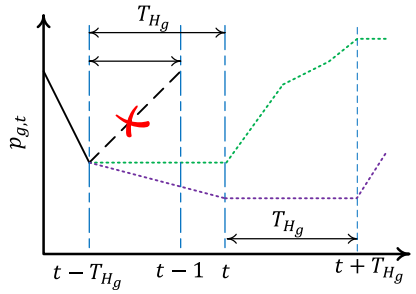

Figure 1. Impact of Xenon-poisoning on nuclear plant's dispatch

Despite the extensive modeling efforts concerning the behavioral constraints of nuclear power plants, relatively few have addressed their unique operational dynamics. Noteworthy examples include the development of a control-oriented state-space model for nuclear reactors, which has demonstrated remarkable accuracy in predicting reactor behavior within predefined operational boundaries [15], [16]. Furthermore, a dynamic model for an integral pressurized water reactor (iPWR)-type SMR was crafted, encompassing detailed reactor core models and associated components [17]. With a focus on the design limitations of SMRs, a study evaluated the feasibility of SMRs operating in tandem with a co-located photovoltaic (PV) plant to support both planned and unplanned load-following and frequency regulation services [18]. Additionally, a unit commitment model was proposed to optimize the utilization of nuclear plants, taking into account peak-valley load regulation services and modeling nuclear fuel consumption through the capacity equity principle [19]. In the context of multi-faceted energy applications, the integration of a steam-bypass process into the SMR model was explored in [20]–[22]. This innovation harnessed high-temperature process heat to produce hydrogen, thereby transforming the SMR model into a versatile energy source. This model closely resembles a traditional steam-turbine-based generator model, but it introduces additional constraints related to regulating bypass steam flow, which, in turn, impact power and reserve schedules.

In previous studies, various approaches have been taken to address xenon-poisoning constraints in the context of nuclear power plant operation. For instance, in [11], xenon-poisoning constraints were developed for a single-run UC-ED operation

model, with a focus on assessing operational flexibility and hold-time durations. However, these models for participating in reserve services closely resembled those of conventional thermal plants, neglecting the specific impact of xenon poisoning on reserve provision. Similarly, in [13], a similar model with xenon-poisoning constraints was employed to analyze the profitability of nuclear plant operations, specifically for load-following services where the nuclear plant was exclusively dedicated to electric power dispatch.

Expanding on this, Poudel and Gokaraju [23] introduced a comprehensive optimization framework for SMRs with xenon-poisoning characteristics. This framework went a step further by integrating SMRs into a renewable-based hybrid energy system, even encompassing a model for a district heating network. It primarily focused on the finer timescale aspects of operation, such as load-following and frequency regulation. Our previous study [24] has explored the dynamics of a nuclear-hybrid renewable energy system within a multi-timescale electricity market operation framework. In this scenario, a district heating network was supplied with heat from a gas-cooled SMR's exhaust, resembling the operational characteristics of a conventional thermal power plant.

However, these prior studies largely treated nuclear plants as conventional thermal plants in the realm of power system operation, limiting the modeling of plant characteristics to conventional constraints. This approach resulted in an operational profile for nuclear power plants that closely mirrored that of traditional power plants. A more comprehensive modeling effort is required to account for the full spectrum of multi-timescale operation. In this study, we have developed an extensive steady-state model tailored specifically for SMRs, making it well-suited for a multi-cycle power system operation framework. Our approach departs from generic constraints and, instead, focuses on the progressive refinement of operational constraints, encompassing coarser and finer timescales. This model accounts for a real-time unit-commitment cycle and incorporates a day-ahead forward electricity market model,which precedes the final real-time economic dispatch model. The significant contributions of this work encompass:

- We've created an all-encompassing multi-timescale steady-state simulation model tailored specifically for SMRs. This model offers an accurate and detailed representation of SMR operational characteristics across a range of timescales, contributing to a deeper understanding of their dynamic behavior.
- Our work intricately outlines the progression of xenon-poisoning constraints as we transition between different timescales. It takes into account the seamless transfer of ramping status from one sub-model to the next, providing a comprehensive view of how SMR behavior evolves under varying operational conditions.
- We have developed new reserve provision rules that consider the dynamic ramping statuses of SMRs. These rules optimize the allocation of capacity for reserve services while factoring in the impact of xenon-poisoning constraints.
- Aside from the details of the nuclear plant modeling, the scope of the multi-timescale study framework has been enhanced to further extent through the inclusion of the capacity expansion planning stage. This stage involves the determination of new resource deployment through rigorous planning studies, which are subsequently validated by detailed operational analyses.

The rest of the paper is organized as follows. Section II establishes the foundational framework for the study and delves into the critical task of determining the optimal size for SMRs. Section III introduces the detailed modeling approach for SMR's multi-timescale simulations. Section IV presents the study cases and results derived from our analysis of SMR's multi-timescale operation. Conclusions and future work are discussed in Section V.

II. Foundational Framework and Model Development

This research involves a coordinated operational analysis with a specific focus on the operational specifics of SMRs. The planning phase of this study leverages an open-source capacity expansion planning tool. Subsequent to the determination of long-term planning decisions, the projected capacity and chosen construction sites are integrated into a multi-timescale energy scheduling and dispatch tool, known as the Flexible Energy Scheduling Tool for Integrating Variable Generation (FESTIV) [25]. FESTIV comprises two distinct modes: the formulation mode, responsible for tasks like modeling plant characteristics and crafting optimization models, and the functional mode, which handles the pre-processing and post-processing of optimization model inputs and outputs. Within this functional mode, specific operational procedures are executed in alignment with the operation policy adopted by the system operator.

The overall study framework, as depicted in Fig. 2, comprises three essential components: a day-ahead Reserve-constrained unit commitment (DARCUC) model, a real-time reserve-constrained unit commitment (RTRCUC) model, and a real-time reserve-constrained economic dispatch (RTRCED) model. This comprehensive framework mirrors the full spectrum of scheduling and dispatch activities typically carried out by an Independent System Operator (ISO) within a deregulated electricity market. Fig. 3 provides an overview of various time-related settings, encompassing factors like the length of the optimization horizon, advisory time duration, and intervals for executing the optimization model within these sub-models. The specifications of the SMR operational parameters are established based on publicly available sources and existing literature [26], [27]. In selecting the parameters, only specifications from similar Pressurized Water Reactor (PWR) based nuclear plants have been considered as references. Values that comply with safety limits have been utilized. Key parameters pertinent to SMR operation are detailed in Table I.

Reserve requirements are determined by following the default FESTIV reserve rule [25], where the regulation reserve varies with the system load and other reserves are set at some fixed values. In this research, we have examined four categories of reserves: regulation-up reserves, regulation-down reserves, spinning reserves, and non-spinning reserves. To

Table I
KEY SMR PARAMETERS

Parameter	Value
Capacity	P^{max}_{SMR}= 50 MW; P^{min}_{SMR}= 7.82 MW
Ramp rate	R^{U}_{SMR}=R^{D}_{SMR}=1.25 MW/min;
Start-up & shut-down time	TUP_{SMR}=TDP_{SMR}=12 h

gain a comprehensive understanding of SMRs' involvement in reserve provision, we have included regulation-down reserves in the array of reserve products. The prioritization of these reserves is determined by comparing the value of insufficient reserves (VOIR) and their activation time. The participation of generators in supplying these various reserves is contingent on their operational characteristics. Table II provides a summary of the assumed VOIRs, activation times, and system reserve requirements.

Table II
RESERVE SETTINGS

Reserve type	Activation time (mins)	VOIR ($/MW-h)	Requirement (MW)
Regulation-up	5	2,500	10% of total load
Regulation-down	5	2,500	10% of total load
Spinning	10	2,250	950
Non-spinning	30	2,000	1,900

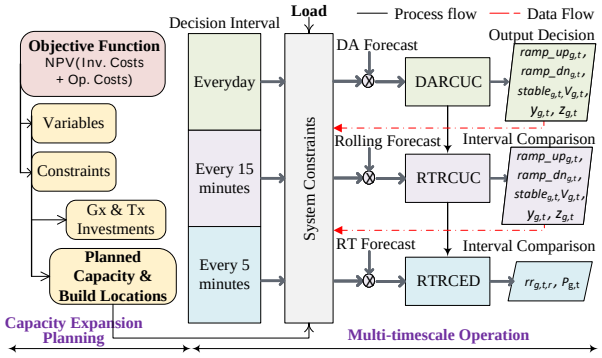

Figure 2. High-level flow diagram of the integrated planning and multi-timescale operation framework employed in this study.

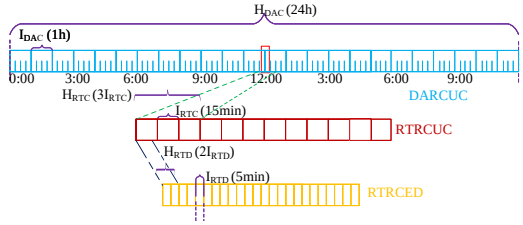

Figure 3. The simulation parameter settings for the multi-timescale model execution.

While the present study attempts to cover a wide timeline, spanning from year-long capacity expansion planning to real-time operation, it does so with certain limitations to maintain scope concentration. Here are some of the primary drawbacks of this study:

- This study has taken an agnostic approach, overlooking the factors influencing the selection of hold-time duration. Our choice of hold-times draws from various durations utilized by operators worldwide [11], inadvertently leaving pertinent factors unaddressed in the decision-making process for hold-time duration.
- In developing the SMR model, we focused on the initial phase of the fuel cycle, where Xenon transient can be compensated by sufficient reactivity. However, the analysis does not account for the transition between different phases of the fuel cycle due to complexities in modeling and computational burdens. Similarly, the capacity expansion study overlooks fuel cycle transitions due to the inherent complexity of integrating time-coupling features, as such studies are conducted on discrete datasets spanning larger time horizons.
- Given the lack of operational data from other SMRs, the validation process of the results primarily relies on a proof of concept through simulation approach.

A. Objective Function & Constraints

The objective function of the multi-timescale energy scheduling and dispatch models is formulated based on the conventional Production Cost Model (PCM), with the aim of minimizing the overall production cost.

$$\textbf{\textit{min}} \ \sum_{t\in T}\Big[\sum_{g\in G}(su_{g,t}+sd_{g,t}+pc_{g,t}+\sum_{r\in RS}rc_{g,t,r}) + \sum_{r\in RS} VOIR_r ir_{t,r} + ls_t\Big] \quad (1)$$

s.t.

$$su_{g,t} \geq SU_g[v_{g,t}-v_{g,t-1}], \forall g\in G, \forall t\in T \quad (2)$$

$$sd_{g,t} \geq SD_g[v_{g,t-1}-v_{g,t}], \forall g\in G, \forall t\in T \quad (3)$$

$$pc_{g,t} = NL_g v_{g,t} + \sum_{k=1}^{K_g} p^k_{g,t} C^k_g, \forall g\in G, \forall t\in T \quad (4)$$

$$rc_{g,t,r} = \sum_{g\in G} rr_{g,t,r} RC_{g,r}, \forall g\in G, \forall t\in T, \forall r\in RS \quad (5)$$

To enforce soft constraints on reserve inadequacy and load-shedding, specific penalty terms like $VOIR$ and ls_t are incorporated. Eq. 1 presents the objective function for the DARCUC sub-model, while the objective functions for the RTRCUC and RTRCED models closely resemble it, with scaling by the respective optimization time resolutions, denoted as I_{RTC} and I_{RTD}. In the context of the RTRCED model, startup and shutdown costs are not considered in the objective function. For brevity, we omit the objective functions of the RTRCUC and RTRCED models, but they can be referenced in [20]. Eqs. 2 and 3 define the startup and shutdown costs, respectively. Eq. 4 represents the production cost while considering the no-load costs, while Eq. 5 defines the reserve cost.

1) Conventional Machine Constraints for SMR and Other Plants: Besides the 'hold-time' constraints modeling, the SMR model is formulated by incorporating a range of conventional but highly detailed plant constraints. These constraints encompass various aspects, such as plant capacity limitations, including constraints related to the cost of generation blocks, minimum allowable up and downtime, operational

restrictions during startup and shutdown in both initial and regular operation phases, limits on available reserve capacity, and constraints governing the maximum number of startup and shutdown operations within the optimization timeframe, among other factors. For an in-depth and comprehensive formulation of these constraints, please refer to [20], [24].

2) System Level Constraints: The system level constraints in the multi-timescale operation model encompass critical factors such as the system-wide energy balance constraint, bus-wise net energy constraint, system-wide reserve constraints, load-shedding limit constraint, and line-flow constraints, among others. Line-flow values are derived using a precomputed power transfer distribution factor (PTDF) matrix. For the sake of brevity, these constraints are not detailed in this paper.

B. Optimal Siting and Sizing of SMR(s)

Since the NREL-118 bus test system does not have a nuclear plant, it is essential to identify the most suitable location and size for the proposed SMR(s) to facilitate an optimal investment decision. To accomplish this, we employed a comprehensive capacity expansion tool called GridPath [28]. GridPath serves as a robust grid analytics platform capable of a wide range of functions, including capacity expansion planning. In the capacity expansion task, GridPath is instrumental in minimizing the total system cost over the planning horizon, taking into account both capital costs (such as generators and transmission lines) and operating costs. The capacity expansion model factors in technical considerations like generator limitations, wind and solar availability, and transmission line capacity across different corridors. Additionally, it incorporates policy constraints such as carbon taxes, renewable energy mandates, and greenhouse gas targets.

For our study, we considered a carbon tax rate of $40 per ton as a pivotal decision-making criterion, along with specific technical constraints and the generic constraints provided by GridPath. Contrary to short-term planning study, long-term planning analysis requires more comprehensive information on the grid infrastructure development policies and high-quality forecasts for renewable generation and electrical load over extended durations. Therefore, we limit our analysis to a five-year short-term capacity expansion study, which, despite its relatively shorter duration, offers foresight suitable for single resource deployments such as SMRs with substantially lower capacities. Our base year was 2020, with the planning horizon extending to the year 2025, aligning with the data used for the multi-timescale operation study in the same year. The choice of an operational study day within this horizon ensures thorough evaluation of investment decisions. By selecting a day from this timeframe, we ensure that prospective variations in load and renewable generation forecasts, along with other relevant input factors, are properly considered in the decision-making process. Cost data, encompassing annualized real cost per MW and variable operation and maintenance costs for various technologies, were sourced from NREL's annual technology baseline archive [29]. Wind sites were selected as candidate locations for SMRs due to their typical positioning further away from densely populated areas, which mitigates safety concerns associated with SMRs. Operational risks are accommodated in the analysis through the plant's capacity factors, assuming the planned or unplanned outages are translated into that parameter.

Fig. 4 illustrates the outcomes of optimal siting and sizing under different decision criteria and additional constraints. Resource deployment decisions are made based on the optimization of the net present value (NPV) of the summation of investment and operation costs, while respecting technical and policy constraints as illustrated in Fig. 2. When transmission line limits are not considered, the model recommends constructing SMRs at multiple locations. However, both the number of SMRs and their locations decrease significantly when transmission limits are factored in. For the sake of precision, the most detailed constraints-driven result, denoted as the $linear\_build$ option in Fig. 4, was adopted as the final decision. Complying with the technical specifications of NuScale's SMR [30], which has a unit size of 50 MW [23], we adjusted the capacity expansion planning decision from 289 MW to a final capacity of 300 MW to be built at Bus-31, resulting in the construction of a total of six SMRs.

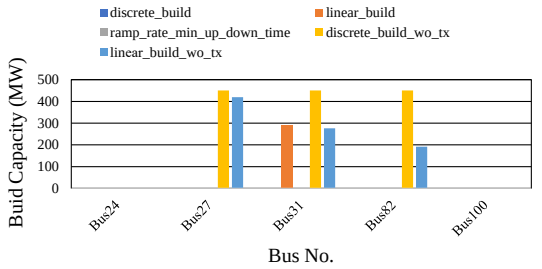

Figure 4. Optimal siting and sizing results for SMRs at various locations in the NREL-118 bus system. The legends indicate the additional constraints considered, in addition to the standard GridPath constraints. (wo = without, tx = transmission)

To further justify the investment decisions on installing the SMRs at the determined location, a cost-benefit analysis has been performed. The cost information is taken from the ATB [29], whereas the benefits are calculated following Eq. 6 [31].

$$Benefit = P_r \frac{\$}{MWh} \times P_o(MW) \times Life(yrs) \times T_{total} \frac{h}{yrs} \quad (6)$$

where P_r is the average price of the electricity product, P_o is the average output of the product, $Life$ is the technical life duration of the SMR, which is 60 years, and T_{total} denotes the active hours of SMRs. To determine these parameter values, the real-time generation and reserve schedules have been used from Case-I (a study case in the current work). To determine the active hours, a 90% capacity factor value has been used as per the ATB database. The average price P_r is calculated by taking the average of the real-time LMPs for both power and ancillary services. The results for the cost-benefit analysis are summarized in Table III, where it shows the benefit-cost ratio is more than 1. Therefore, it can be concluded that the investment decision is justified.

Table III
COST-BENEFIT ANALYSIS RESULTS FOR THE SMR PROJECT

Area	Component	Value
Costs	Overnight Capital Cost ($)	2.24×10^9
	Fixed O&M Cost ($)	2.14×10^9
	Variable O&M Cost ($)	2.31×10^8
	Fuel Costs ($)	8.11×10^8
Benefits	Energy Revenue ($)	5.96×10^9
	Ancillary Service Revenue (Cumulative) ($)	2.69×10^7
Net Benefits ($)	-	4.05×10^8
Benefit-Cost Ratio	-	1.07
Findings	-	cost effective

III. COMPREHENSIVE FORMULATION OF SMR MODELING CONSTRAINTS ACROSS VARIOUS TIMESCALES

In conventional UC-ED simulation studies, nuclear plants are typically regarded as must-run base-load facilities and are, therefore, modeled as conventional generators. This entails imposing constraints to ensure continuous operation and stable output. However, for the purpose of this study, it is essential to account for the flexible operational characteristics of the reactor. Specifically, the presence of fission product poisoning, primarily caused by ^{135}Xe, imposes constraints on the reactor's power output to prevent rapid ramping up immediately after a ramp-down event, as highlighted in [13]. Consequently, the introduction of a time delay before the subsequent ramp up following a ramp-down event becomes a critical aspect of the modeling process. Unlike prior research efforts that predominantly focus on modeling these distinctive traits alone, our study not only addresses these constraints but also elucidates their evolution from broader timescales to finer ones.

A. Day-ahead Reserve-Constrained Unit Commitment

In the DARCUC model, the integrated constraints reflect the broadest operational characteristics. Given the inherently lower operational cost associated with nuclear plants, a 'must-run' constraint has been incorporated, as illustrated in Eq. 7.

$$v_{g,t} = 1, \forall g \in G_{NPP}, \forall t \in T \tag{7}$$

Eq. 8 illustrates the impact of xenon poisoning on nuclear operational maneuvers. It enforces a minimum waiting period of T_H (hold-time) hours following a ramp-down event, during which a ramp-up event is prohibited.

$$\begin{aligned}[ramp\_up_{g,t} - ramp\_up_{g,t-1}] \cdot T_{Hg} = \\ \sum_{\tau=t-T_{Hg}}^{t-1} (stable_{g,\tau} + ramp\_up_{g,\tau}), \\ \forall g \in G_{NPP}, \forall t \in T > T_H\end{aligned} \tag{8}$$

While Eq. 8 alone may not fully capture the impact of fission-product poisoning on nuclear plant operation, it remains the pivotal constraint for modeling this particular characteristic. The binary ramping status variables featured in this equation are incorporated into both the ramping-up and ramping-down constraints (Eqs. 9 & 10), providing guidance for the plant's dispatch level.

$$p_{g,t} - p_{g,t-1} \leq R_g^U \cdot ramp\_up_{g,t}, \forall g \in G_{NPP}, \forall t \in T \tag{9}$$

$$p_{g,t-1} - p_{g,t} \leq R_g^D \cdot ramp\_dn_{g,t}, \forall g \in G_{NPP}, \forall t \in T \tag{10}$$

To maintain the logical coherence of the binary ramping statuses, an equality constraint described in Eq. 11 has been employed to guarantee that only one ramping status is active at any given moment.

$$\begin{aligned}ramp\_up_{g,t} + ramp\_dn_{g,t} + stable_{g,t} = 1, \\ \forall g \in G_{NPP}, \forall t \in T\end{aligned} \tag{11}$$

As the occurrence of a ramp-down event is contingent on the system's demand, it becomes imperative to define constraints that govern its range and trajectories. Given that ramping can occur in both upward and downward directions, it is essential to limit the disparity in dispatch levels between two consecutive time intervals in line with the nuclear plant's ramp-rate, whether ascending or descending. These ramp-rate restrictions should persist as long as the hold-time constraints need to be adhered to following a ramp-down event. To address the initial ramping event that takes place either in the very first hour or before the optimization horizon begins, it becomes necessary to introduce constraints that can accommodate the ramping pattern of the SMR during that initial hour. This is also crucial for conducting multi-horizon simulations where 'hold-time' constraints must be rolled across optimization horizons.

To meet this requirement, Algorithm 1 has been developed for consecutive RTRCUC optimization horizons, presenting an intertemporal coupling mechanism. A similar algorithm has been formulated for the DARCUC cycle, encompassing relevant temporal parameters. However, to maintain brevity in this manuscript, the details of the DARCUC algorithm have been omitted. This choice stems from the perception that the RTRCUC algorithm provides a more comprehensive explanation of intertemporal coupling mechanisms due to its intricate structure. To ensure the xenon-poisoning constraint in effect in the hours between the initial hour and the ramp up off enforcement duration, $T^{R^U_{off}}$, Eq. 12 has been integrated into the unit commitment models. The determination of $T^{R^U_{off}}$ and $U_{g,t}^{R^U_{off}}$ has been explained in Algorithm 1.

$$\begin{aligned}ramp\_up_{g,t} \leq U_{g,t}^{R^U_{off}}, \\ \forall g \in G_{NPP}, \forall t \in [1, min(H_{DAC}, T_i^{R^U_{off}})]\end{aligned} \tag{12}$$

1) Ancillary Services (Reserves) Capability Constraints: As the operational characteristics of an SMR plant with an active xenon-poisoning constraint differ from those of conventional synchronous generating plants, it is necessary to formulate constraints for ancillary services (reserves) provision that account for these technical limitations. One of our key arguments suggests that the reserve capacity of an SMR is

influenced by its stable operational state. While an SMR can indeed supply upward and downward reserves during ramping up and ramping down, respectively, the magnitude of reserve provision is constrained by its ramping rate capacity. However, when it is in a stable state, it can be argued that SMRs are unable to provide any reserves. To establish the upper and lower limits for reserve provision in light of this argument, we illustrate the reserve provision constraints when supplying upward and downward reserves in Eqs. 13 and 14.

$$\sum_{r} rr_{g,t,r}/RAT_r \cdot RON_r \leq (1 - stable_{g,t}) \cdot RR_g, \quad \forall r \in RS; R_{dir} = up \tag{13}$$

$$\sum_{r} rr_{g,t,r}/RAT_r \cdot RON_r \leq (1 - stable_{g,t}) \cdot RR_g, \quad \forall r \in RS; R_{dir} = down \tag{14}$$

2) Alternative Reserve Provision Scheme: The argument against the prohibition of ancillary reserves at stable status is that the unit can still ramp down while in a stable state. In response to this, an alternative reserve provision scheme can be formulated based on the following principles:

- When in a stable state, only downward reserves are available.
- When in a ramp-up state, only upward reserves are available.
- When in a ramp-down state, only downward reserves are available.

Considering all the aforementioned principles, the reserve provision constraints can be formulated as follows.

$$\sum_{r} rr_{g,t,r}/RAT_r \cdot RON_r \leq ramp\_up_{g,t} \cdot RR_g, \quad \forall r \in RS; R_{dir} = up \tag{15}$$

$$\sum_{r} rr_{g,t,r}/RAT_r \cdot RON_r \leq (1 - ramp\_up_{g,t}) \cdot RR_g, \quad \forall r \in RS; R_{dir} = down \tag{16}$$

B. Real-time Reserve-Constrained Unit Commitment

Because ramping-down is not a commitment decision and occurs quite quickly, the decision to ramp down made in the DARCUC cycle may not necessarily impact the ramping-down decisions to be made in the RTRCUC cycle. Situations may arise where there is a ramp-down event in the DARCUC cycle, but none in the RTRCUC cycle. However, a ramp-down event in the RTRCUC cycle itself requires compliance with the 'hold-time' constraint in the same or immediate subsequent RTRCUC cycles.

The RTRCUC formulation for SMR characteristics predominantly focuses on representing the potential transitions in its ramping status. These constraints guide the SMR to maintain its stable status or ramp up or down, depending on its ramping status at the beginning of the RTRCUC update interval, while also respecting any binding status carried over from the coarser DARCUC decisions.

$$[ramp\_up_{g,t} - ramp\_up_{g,t-1}] \cdot T_{Hg}/I_{RTC} \leq \sum_{\tau=t-T_{Hg}/I_{RTC}}^{t-1} (stable_{g,\tau} + ramp\_up_{g,\tau}), \quad \forall g \in G_{NPP}, \forall t \leq T - T_H/I_{RTC} + 1 \tag{17}$$

$$[ramp\_up_{g,t} - ramp\_up_{g,t-1}] \cdot (T - t + 1) \leq \sum_{\tau=t}^{T} (stable_{g,\tau} + ramp\_up_{g,\tau}), \quad \forall g \in G_{NPP}, \forall t > T - T_H/I_{RTC} + 2 \tag{18}$$

The formulation of constraints to account for the xenon-poisoning effect on consecutive ramping statuses is akin to the DARCUC model, with the key difference lying in the time domain due to the configuration of the optimization time slots. Eqs. 17 and 18 illustrate the characteristics of ramping status transitions within the RTRCUC time slot, which is divided into two segments in this case to accommodate potential changes in ramping status occurring at different time intervals within the RTRCUC timeframe. The equations governing ramping up and ramping down during the initial hours are similar to those seen in Eq. 9 and Eq. 10, with the only modification being the inclusion of an additional factor representing the RTRCUC time interval multiplied by the ramp-rate. The equality constraint involving all three ramping status variables remains consistent in RTRCUC.

The ramp-up and ramp-down constraints for both DARCUC and RTRCUC during the initial intervals are alike, differing only in the length of the time interval (represented as a multiplying factor on the right-hand side). These constraints, when incorporated, place limits on the initial dispatch level of the nuclear plant based on the previous ramping status, in addition to the regular ramping constraints.

To ensure the implementation of a carried-over stable status, a constraint similar to Eq. 12 is also integrated into the RTRCUC model. The process of how ramping statuses are transitioned and how dispatch decisions are influenced by them is explained Algorithm 1 to maintain coherence across successive RTRCUC optimization horizons.

Algorithm 1 Intertemporal coupling algorithm for enforcing ramp-up off decisions in intervals subsequent to a ramp-down event across RTRCUC sub-models

for i=1:n_{NUC} **do**
  Determine the initial timestamp of SMR dispatch schedule check for ramp-down $t_{start}^{R_D} = max(1, floor(t_{RTRCUC} - T_{H_i} \times I_{RTC}))$.
  Select the SMR dispatch schedules from $t_{start}^{R_D}$ to the current timestamp t_{RTRCUC}.
  Determine the incremental or decremental changes (Δp_i^{NUC}) in SMR dispatch in the selected timestamps.
  if $all(\Delta p_i^{NUC}) \geq 0$ **then**
    Set ramp-up off enforcement status, $U_{i,t}^{R_{off}^U} = 1; \forall t \in [1, H_{RTC}]$.
  else
    Find the timestamp index, $t_{last}^{R^D}$ of the last decrement where, $\Delta p_i^{NUC} < 0$.
    Determine the duration of ramp-up off enforcement, $T_i^{R_{off}^U} = T_H \times I_{RTC} - ((t_{RTRCUC} - t_{start}^{R_D}) - t_{last}^{R^D})$
    Set ramp-up off enforcement status, $U_{i,t}^{R_{off}^U} = 0; \forall t \in [1, min(H_{RTC}, T_i^{R_{off}^U})]$.
  end if
end for

C. Real-time Reserve-Constrained Economic Dispatch

Compared to the formulations of the DARCUC and RTRCUC models, the RTRCED model requires fewer constraints to accommodate the xenon-poisoning impact. This is because unit statuses and ramping statuses are already determined through the execution of the DARCUC and RTRCUC models. Therefore, the constraints are primarily designed to guide the dispatch levels, encompassing the provision of reserves, for each of the available units. Eqs. 19 and 20 illustrate how the dispatch level of the nuclear plant evolves from one interval to the next, while considering its ramping limit and the pre-established ramping statuses in the corresponding intervals.

$$\begin{aligned} p_{g,t} - p_{g,t-1} \leq R_g^U \cdot ramp\_up_{g,t} \cdot 60 \\ \cdot I_{RTD} \cdot (stable_{g,t} - stable_{g,t-1}), \\ \forall g \in G_{NPP}, \forall t > 1, \forall stable_{g,t} > stable_{g,t-1} \end{aligned} \tag{19}$$

$$\begin{aligned} p_{g,t} - p_{g,t-1} \leq R_g^U \cdot ramp\_up_{g,t} \cdot 60 \\ \cdot I_{RTD} \cdot (stable_{g,t-1} - stable_{g,t}), \\ \forall g \in G_{NPP}, \forall t > 1, \forall stable_{g,t} < stable_{g,t-1} \end{aligned} \tag{20}$$

Similar equations are also incorporated for ramping-down scenarios. To reflect the carry-over behavior of stable ramping status on the dispatch level, Eq. 21 has been formulated.

$$\begin{aligned} p_{g,t} - p_{g,t-1} = 0, \\ \forall g \in G_{NPP}, \forall t > 1, \forall stable_{g,t} = stable_{g,t-1} = 1 \end{aligned} \tag{21}$$

IV. Case Study and Results

A. Experimental Setup

In order to showcase the adaptability of the SMR model, SMRs are integrated into the NREL-118 bus test system, each with varying hold-time and reserve regulations. The choice of the NREL-118 bus system is attributed to its notable high utilization of renewable energy sources, making it a suitable hypothetical scenario for assessing how SMRs influence the operational characteristics of the system. This system comprises 17 wind farms, accounting for approximately 4.38% of the installed capacity, and 75 photovoltaic (PV) plants, representing around 14% of the installed capacity. While developing the test case, the detailed generation constraints such as up and down ramping, minimum generation level, heat rate, fuel use, etc. have been considered. Additionally, year-long time-synchronous data has been provided for day-ahead and real-time renewable generation and electricity load forecasts, facilitating the examination of seasonal variations in system operation. The test data are arranged to represent the three regions in the test system along with the detailed transmission representation of buses and transmission lines. This comprehensive approach to modeling, encompassing nearly every network component, renders the test case more realistic than other standard test data available.

To align with the outcomes of capacity expansion planning, the six SMRs are linked to Bus no. 31, employing the appropriate generator participation factors and generator-bus mapping procedures. Moreover, to ensure precise alignment with weather conditions, we integrate both day-ahead and real-time predictions regarding renewable generation and load into the multi-timescale model. These forecasts are sourced from the NREL-118 bus system repository [32]. In contrast, the forecasts needed to run the RTRCUC model are generated by the FESTIV forecast engine.

In order to demonstrate the adaptability of the proposed multi-timescale modeling approach for 'fission-product poisoning' characteristics, it becomes imperative to explore how different choices in 'hold-time' impact the involvement of SMRs in both the energy and ancillary reserve markets. The selection of 'hold-time' durations aligns with established practices among nuclear plant operators [11]. Furthermore, the simulation was conducted over the course of a full day to comprehensively analyze the operational characteristics of the proposed plant, capturing variations in load during peak and off-peak hours, as well as fluctuations in renewable generation. Additionally, it's crucial to assess how alterations in market structure affect SMRs' participation, their resulting operational benefits, and the flexibility margin within the overall system operation. Given our confinement of making ramping status decisions to the DARCUC and RTRCUC timescales, it is reasonable to focus our examination on these specific timescales.

In order to examine the aforementioned impacts, three case studies are proposed.

- Case I: Hold-time $T_H = 2h$, with reserve provision regulated by stable status.
- Case II: Hold-time $T_H = 2h$, with reserve provision regulated by ramp-up status.
- Case III: Hold-time $T_H = 3h$, with reserve provision regulated by ramp-up status.
- Case IV (base case): Hold-time $T_H = 0h$ and $P_g^{min} = 0MW$ (the most flexible case).

Among the aforementioned case studies, the first two cases delve into examining how different choices in reserve rules impact the operation of the system, while the third case focuses on investigating how adjustments to the duration of the 'hold-time' affects both the operation of SMRs and the overall system.

To manage computational costs, the simulations are limited to a single daytime horizon. Specifically, the simulations cover the entire day of January 1st, 2025, aligning with the capacity expansion planning decisions for that year. The three-cycle optimization models are constructed using GAMS 32.2 and are solved using ILOG CPLEX 12.8. All simulations are executed on a high-performance computing facility known as Ganymede [33], employing 40 processors and 64GB of memory. Input and output data processing are facilitated through the MATLAB interface of FESTIV.

B. Results and Discussion

To assess how various selections of hold-time and reserve rules impact the operation of the multi-timescale system, we have examined the resulting generation and reserve schedules. Additionally, to gauge the extent of operational flexibility when SMRs interact with the rest of the NREL-118 bus grid, we have documented the curtailment of renewable energy. This data is then compared with the base case, which represents the full flexible operation of SMRs without any hold-time and minimum generation restrictions.

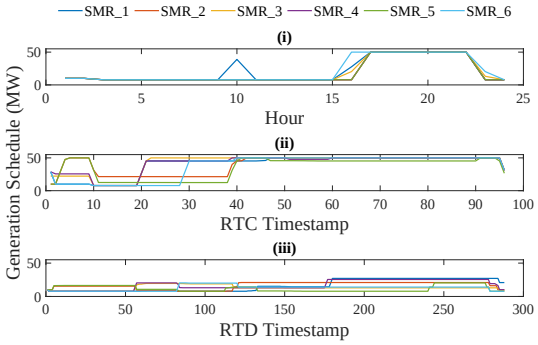

Figure 5. Generation schedules of SMRs in (i) DARCUC, (ii) RTRCUC, and (iii) RTRCED cycles for Case I.

Fig. 5 displays the generation patterns of the six SMRs in Case I across all three examined cycles. During the DARCUC cycle, the SMRs exhibit a trend of generating more power during the late peak hours as opposed to the early peak hours and regular hours. This phenomenon is a result of constraints on generating resources during the late peak hours when fewer cost-effective generating alternatives are available. Similar generation trends are observable in the RTRCUC and RTRCED cycles. However, in the RTRCUC cycle, with the exception of a few early hours, all SMRs commit to delivering their maximum capacity in the later hours, driven by the same factors observed in the DARCUC cycle.

In the RTRCED cycle, similar generation patterns are also evident but with reduced generation margins. This can be attributed to the presence of more cost-effective generating resources and relatively higher incentives for reserves. Across all the generation profiles, it is worth noting that the minimum 2-hour hold-time restriction before a ramp-up event following a preceding ramp-down event is consistently upheld. Seasonal load variation impacts the SMR generation schedules greatly, and it has been observed from a summer day simulation (July 1st) where more ramping up and down events occur due to the higher system load variation. This phenomenon is illustrated in Fig. 6 where some of the SMRs seem to undergo more ramping up and down process compared to the current winter day simulation (for brevity only the DA generation schedules are presented).

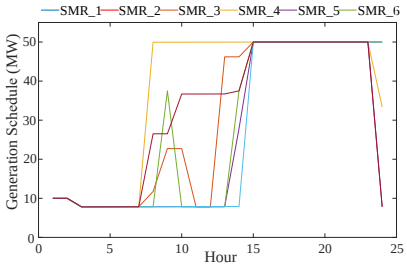

Figure 6. SMR generation schedules for July 1st in the DA cycle.

Fig. 7 presents the schedules for spinning reserves provided by the SMRs. In the DARCUC and RTRCED cycles, spinning reserves are predominantly scheduled to be supplied during peak hours. However, in the RTRCUC cycle, SMRs exhibit consistent participation in supplying spinning reserves from early to mid-day hours. This particular spinning reserve pattern in the RTRCUC cycle is influenced by the available capacity of the SMRs during those specific hours.

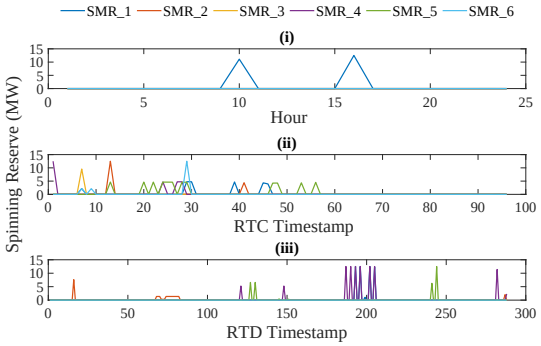

Figure 7. Spinning reserve schedules of SMRs in (i) DARCUC, (ii) RTRCUC, and (iii) RTRCED cycles for Case I.

When examining Fig. 8, it becomes evident that SMRs have a higher level of involvement in providing both regulation-up and regulation-down reserves compared to spinning reserves. This trend can be attributed to the relatively higher values of $VOIR$ and reserve prices. Notably, in Case I, there is a restriction on the allocation of reserves during the stable status of operation, resulting in no reserve allocation during specific hours, i.e., around 8th-9th and 20th-22nd hours.

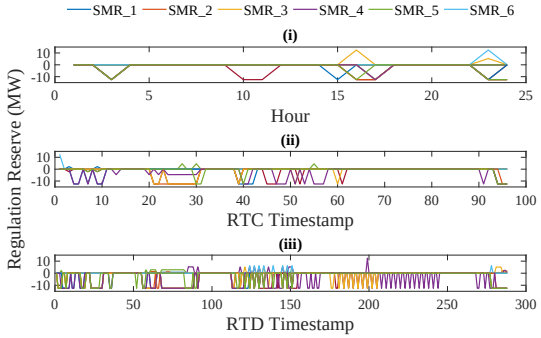

Figure 8. Regulation reserve schedules of SMRs in (i) DARCUC, (ii) RTRCUC, and (iii) RTRCED cycles for Case I.

The generation profiles depicted in Fig. 9 for Case II exhibit patterns akin to those observed in Case I, although with relatively less variability. In Case II, similar to Case I, the SMRs reach their maximum capacity during evening peak hours, but there is more available generation capacity compared to Case I. This extensive utilization of generation capacity in Case II leaves limited room for reserve allocations in real-time cycles, as illustrated in Figs. 10 and 11.

In the DARCUC cycle, reserve allocation is observed to be more adaptable for spinning reserves and regulation-up reserves. This highlights the differences in reserve rules between Case I and Case II, particularly in terms of the provision of reserves during the hours where reserve allocation was prohibited in Case I (around 8th-9th and 20th-22nd hours). When examining all the reserve profiles in Case II, it becomes evident that the reserve rules implemented in Case II are more restrictive compared to those in Case I. This increased constraint is due to the reliance on multiple ramping status variables. Consequently, the more stringent reserve rules exert a more pronounced influence during real-time cycles, where decision-making horizons are shorter in duration. This is the underlying reason why, in Case II, the SMRs opt to generate more power rather than allocating their capacity for reserves.

In Case III, we maintain the same reserve rule as in Case II,

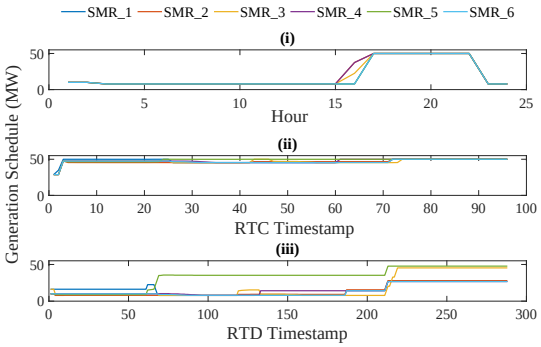

Figure 9. Generation schedules of SMRs in (i) DARCUC, (ii) RTRCUC, and (iii) RTRCED cycles for Case II.

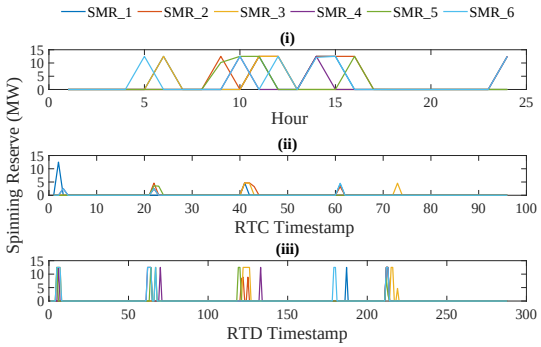

Figure 10. Spinning reserve from SMRs in (i) DARCUC, (ii) RTRCUC, and (iii) RTRCED cycle for Case II.

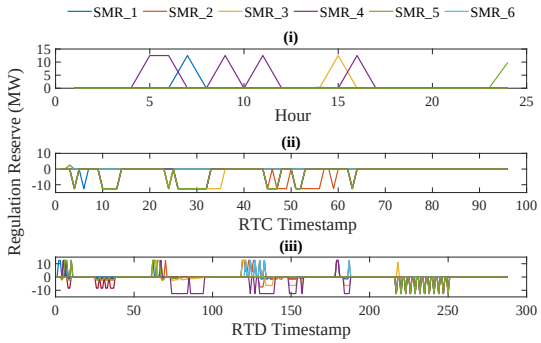

Figure 11. Regulation reserve from SMRs in (i) DARCUC, (ii) RTRCUC, and (iii) RTRCED cycle for Case II.

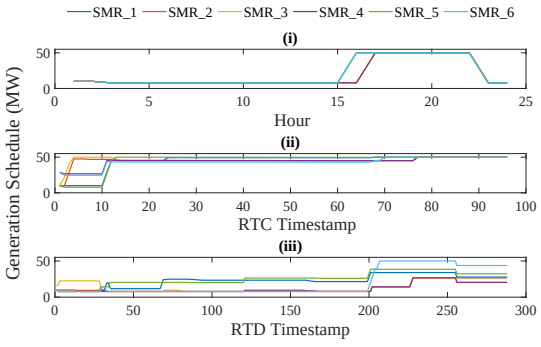

Figure 12. Generation schedules of SMRs in (i) DARCUC, (ii) RTRCUC, and (iii) RTRCED cycles for Case III.

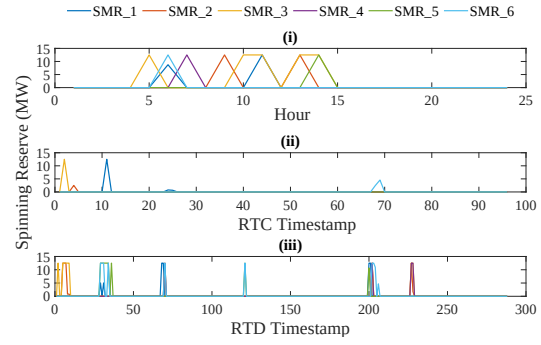

Figure 13. Spinning reserve schedules from SMRs in (i) DARCUC, (ii) RTRCUC, and (iii) RTRCED cycles for Case III.

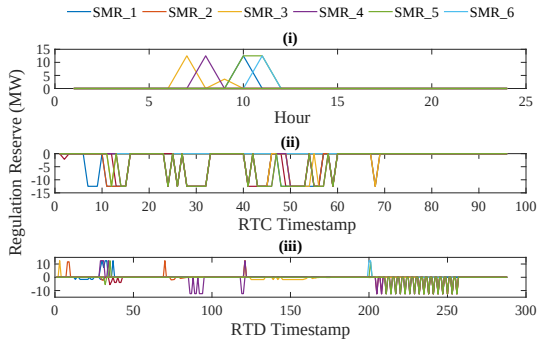

Figure 14. Regulation reserve schedules from SMRs in (i) DARCUC, (ii) RTRCUC, and (iii) RTRCED cycles for Case III.

but we extend the hold-time restriction to 3 hours to examine the effects of longer hold-time and a more cautious operational approach. The generation profiles depicted in Fig. 12 exhibit patterns that are more akin to those seen in Case II across all three cycles. However, it's important to note that the ramping patterns are more constrained in Case III due to the extended hold-time restriction on subsequent ramp-ups. This becomes evident when analyzing the early-hour generation profiles of SMRs.

The spinning reserve profiles, depicted in Fig. 13, reveal significantly lower involvement of SMRs in the DARCUC cycle, while in the real-time cycles, their participation is nearly alike. A similar trend is also noticeable in the allocation of regulation reserves, as shown in Fig. 14. This observation supports the notion that the extended hold-time duration has a more restraining effect on reserve allocation in the broader timescale of the DARCUC cycle.

To assess and quantify the comparative advantages of the previously mentioned cases, they are compared with a highly flexible operational case that imposes no hold-time, minimum generation, or ramping restrictions. It's worth noting that this extreme mode of operation is not typically adopted by real-world operators, but it serves as a reference point for measuring deviations from an unrestricted operational mode.

Fig. 15 illustrates the generation profiles, while Figs. 16 and 17 present the spinning and regulation reserve profiles, respectively, for this unrestricted mode of operation. In this operational mode, the SMRs respond to the system's requirements in an exceptionally flexible manner, characterized by their highest contribution in the reserve market, particularly during the real-time cycles where operational flexibility is most crucial.

To present a more clarified numerical comparison of different cases in terms of reserve provision, Table IV is presented with the cumulative reserve provisions in different cycles. The data presented in Table IV reveals that all the cases with consecutive ramp-down restrictions have allocated sig-

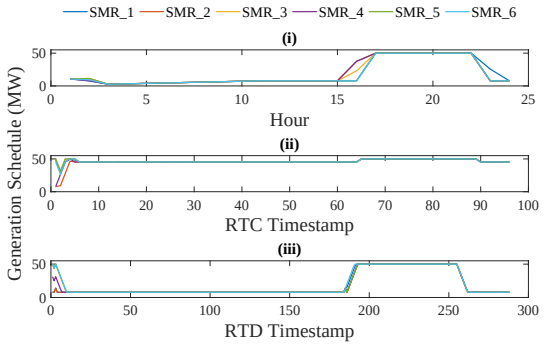

Figure 15. Generation schedules of SMRs in (i) DARCUC, (ii) RTRCUC, and (iii) RTRCED cycles for Case IV (base case).

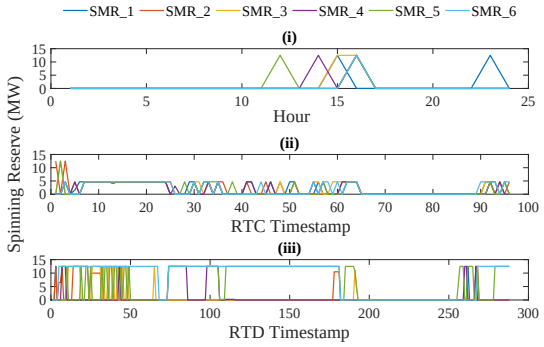

Figure 16. Spinning reserve schedules from SMRs in (i) DARCUC, (ii) RTRCUC, and (iii) RTRCED cycles for Case IV.

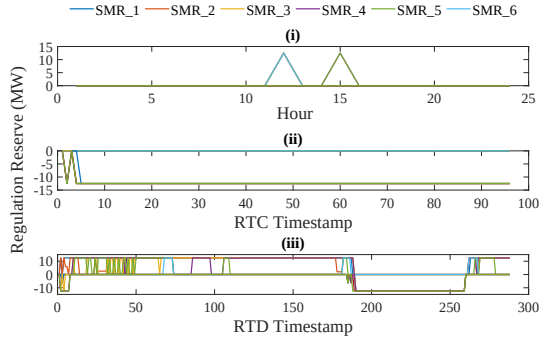

Figure 17. Regulation reserve schedules from SMRs in (i) DARCUC, (ii) RTRCUC, and (iii) RTRCED cycles for Case IV.

nificantly less reserve capacity when compared to the most flexible Case IV. Among all four cases, Case III stands out with the lowest amount of reserves allocated, underscoring the substantial effect of extended hold-time restrictions on the ramping capacity of SMRs.

Furthermore, in Cases I and II where there is a 2-hour hold-time restriction, the reserve rule based on the stable status has enabled a higher allocation of reserve capacity in comparison to the reserve rule based on the ramp-up status.

In terms of revenue generation, as shown in Table V, Case I emerges as the most profitable operational scheme. This revenue metric is calculated based on earnings exclusively in the DARCUC and RTRCED cycles. The process involves multiplying the nodal LMPs with scheduled energy and ancillary reserves, along with their respective nodal marginal prices, for both the day-ahead and real-time cycles. These values are then summed up to calculate the gross revenue. Therefore, in terms of both electricity production and ancillary services, Case I yields a more financially beneficial operation in these two cycles, despite not utilizing the maximum available resources.

Table IV
CUMULATIVE RESERVE PROVISION PROFILES OF SMRS

Case	Reserve	DARCUC (MWh)	RTRCUC (MWh)	RTRCED (MWh)
I	Reg-up	25.03	8.77	8.73
	Reg-down	350	333.80	312.50
	Spinning	34.06	66.37	19.36
II	Reg-up	97.70	1.25	30.20
	Reg-down	0	384.37	40.42
	Spinning	334.84	19.93	18.75
III	Reg-up	78.59	0	14.64
	Reg-down	0	456.79	12.36
	Spinning	146.25	8.97	27.01
IV	Reg-up	75	0	379.56
	Reg-down	0	1,753.10	21.87
	Spinning	125	261.42	189.18

Table V
EARNED REVENUES BY THE SMR UNITS

Case	Revenue ($)	$\Delta(\%)$
I	27,210	+4.14
II	26,741	+2.35
III	27,115	+3.78
IV	26,124	base

Another measure of operational flexibility is the curtailment of renewable energy within the system, as outlined in Table VI. While the cumulative installed capacity of SMRs is relatively small in comparison to the entire system capacity, the slight differences among the considered cases signify their current and potential future impact as SMRs are deployed on a larger scale. As expected, Case IV, with its highly flexible operational approach, incurs the least amount of curtailment. In contrast, curtailment levels are quite similar and higher than the base case for the other three cases, indicating that their capacity falls significantly short of making a substantial difference in this regard. The proposed SMRs have more ramping capability due to its comparatively higher band of ramping. This feature makes it preferable to be adopted in a power system with abundance of volatile renewable resources. Higher ramping capability also allows to provide more ancillary reserves which increases the security of operation. It's intuitive that these SMRs may earn less from energy trading compared to the conventional nuclear plants operating at nearly rated capacity [34], but can be more profitable if their contribution to operation flexibility and security are evaluated with proper metrics.

Table VI
RENEWABLE GENERATION CURTAILMENT

Case	Curtailment (MWh)	$\Delta(\%)$
I	10.884	+34.20
II	10.888	+34.23
III	10.885	+34.20
IV	8.111	base

V. Conclusion

In this research, we have developed a comprehensive steady-state model for Small Modular Reactors (SMRs) to investigate their influence on the multi-timescale operation of the power system. Before incorporating SMRs into the multi-timescale operation model, we conducted a multi-year capacity expansion study to assess the optimal location(s) and size(s) for SMRs. In addition to the standard plant constraints, we adapted "hold-time" constraints for various sub-models at different timescales. We also formulated necessary constraints to ensure smooth transitions between consecutive sub-model simulations.

We devised and evaluated two distinct reserve provision rules for SMR operations across different timescales. The duration of the "hold-time" was found to impact the coarser timescale operation of SMRs, while the reserve rule significantly influenced the finer timescale operation. Specifically, the reserve rule guided by the ramp-up status was more restrictive in terms of power and reserve provision, while the stable status-guided reserve rule generated more revenue but led to nearly the same amount of renewable energy curtailment as the ramp-up status-guided reserve rule.

Looking ahead, we plan to conduct a study involving co-located renewable resources at SMR sites to gain a more localized understanding of operational flexibility. To better evaluate the true value of flexible SMR operation and ensure a more favorable energy and ancillary service market, we will redesign and reevaluate the value metrics. Additionally, we will explore the impact of different optimization horizon lengths on operational flexibility and embark on an evaluation and comparison of various SMR technologies.

Acknowledgment

This material is based upon work supported by the U.S. Department of Energy under Award No. DE-NE0008899 and Award through the INL Laboratory Directed Research & Development (LDRD) Program under DOE Idaho Operations Office Contract DE-AC07-05ID14517.

References

[1] S. Patel, "Flexible operation of nuclear power plants ramps up," [Online] Available at: https://www.powermag.com/flexible-operation-of-nuclear-power-plants-ramps-up, April 1, 2019.

[2] D. Michaelson and J. Jiang, "Review of integration of small modular reactors in renewable energy microgrids," *Renewable and Sustainable Energy Reviews*, vol. 152, p. 111638, 2021.

[3] P. Maloney, "How market forces are pushing utilities to operate nuclear plants more flexibly," [Online]Available at: https://www.utilitydive.com/news/how-market-forces-are-pushing-utilities-to-operate-nuclear-plants-more-flex/427496, [Accessed: 04 Oct. 2023].

[4] M. Cooper, "Small modular reactors and the future of nuclear power in the united states," *Energy Research & Social Science*, vol. 3, pp. 161–177, 2014.

[5] U.S.NRC, "List of Power Reactor Units," [Online] Available at: https://www.nrc.gov/reactors/operating/list-power-reactor-units.html.

[6] NuScale, "Small modular reactor," [Online] Available at: https://www.nuscalepower.com/-/media/nuscale/pdf/fact-sheets/smr-fact-sheet.pdf, [Accessed: 23 Feb. 2024].

[7] M. Hundt, R. Barth, N. Sun, S. Wissel, and A. Voß, "Compatibility of renewable energies and nuclear power in the generation portfolio: Technical and economical aspects," 2009.

[8] H. Ludwig, T. Salnikova, A. Stockman, and U. Waas, "Load cycling capabilities of german nuclear power plants (NPP)," *VGB powertech*, vol. 91, 2011.

[9] P. Morilhat, S. Feutry, C. Lemaitre, and J. M. Favennec, "Nuclear power plant flexibility at EDF," *VGB PowerTech*, vol. 99, no. 5, pp. 32–41, 2019.

[10] HyperPhysics, "Xenon poisoning," [Online] Available at: http://hyperphysics.phy-astr.gsu.edu/hbase/NucEne/xenon.html.

[11] J. D. Jenkins, Z. Zhou, R. Ponciroli, R. B. Vilim, F. Ganda, F. de Sisternes, and A. Botterud, "The benefits of nuclear flexibility in power system operations with renewable energy," *Applied energy*, vol. 222, pp. 872–884, 2018.

[12] NuScale, "NuScale SMR Technology: An Ideal Solution for Repurposing U.S. Coal Plant Infrastructure and Revitalizing Communities," [Online] Available at: https://www.nuscalepower.com/-/media/nuscale/pdf/publications/nuscale-smr-technology-an-ideal-solution-for-coal-plant-replacement.pdf, [Accessed: 23 Feb. 2024].

[13] R. Ponciroli, Y. Wang, Z. Zhou, A. Botterud, J. Jenkins, R. Vilim, and F. Ganda, "Profitability evaluation of load-following nuclear units with physics-induced operational constraints," *Nuclear Technology*, vol. 200, no. 3, pp. 189–207, 2017.

[14] Z. Zhou, J. D. Jenkins, A. Botterud, R. Ponciroli, and F. Ganda, "Modeling nuclear power as a flexible resource for the power grid," *FERC*, 2020.

[15] A. Gábor, C. Fazekas, G. Szederkényi, and K. M. Hangos, "Modeling and identification of a nuclear reactor with temperature effects and xenon poisoning," *European jour. of control*, vol. 17, no. 1, pp. 104–115, 2011.

[16] M. Mangold, "Discussion on:"modeling and identification of a nuclear reactor with temperature effects and xenon poisoning," *European J. of Control*, vol. 17, no. 1, pp. 116–119, 2011.

[17] B. Poudel, K. Joshi, and R. Gokaraju, "A dynamic model of small modular reactor based nuclear plant for power system studies," *IEEE Transactions on Energy Conversion*, vol. 35, no. 2, pp. 977–985, 2019.

[18] K. Joshi, B. Poudel, and R. Gokaraju, "Investigating small modular reactor's design limits for its flexible operation with photovoltaic generation in microcommunities," *Journal of Nuclear Engineering and Radiation Science*, vol. 7, no. 3, p. 031303, 2021.

[19] Y. Xu, Z. Wang, W. Sun, S. Chen, Y. Wu, and B. Zhao, "Unit commitment model considering nuclear power plant load following," in *2011 International Conference on Advanced Power System Automation and Protection*, vol. 3. IEEE, 2011, pp. 1828–1832.

[20] J. Rahman, R. Jacob, and J. Zhang, "Multi-timescale power system operations for electrolytic hydrogen generation in integrated nuclear-renewable energy systems," *TechRxiv*, 2023.

[21] R. A. Jacob and J. Zhang, "Modeling and control of nuclear–renewable integrated energy systems: Dynamic system model for green electricity and hydrogen production," *Journal of Renewable and Sustainable Energy*, vol. 15, no. 4, 2023.

[22] B. Poudel, M. Gautam, B. Li, J. Huang, and J. Zhang, "Design, modeling and simulation of nuclear-powered integrated energy systems with cascaded heating applications," *Journal of Renewable and Sustainable Energy*, vol. 15, no. 5, 2023.

[23] B. Poudel and R. Gokaraju, "Optimal operation of SMR-RES hybrid energy system for electricity & district heating," *IEEE Transactions on Energy Conversion*, 2021.

[24] J. Rahman and J. Zhang, "Multi-timescale operations of nuclear-renewable hybrid energy systems for reserve and thermal product provision," *Journal of Renewable and Sustainable Energy*, vol. 15, no. 2, 2023.

[25] E. Ela, B. Palmintier, I. Krad *et al.*, "FESTIV (Flexible energy scheduling tool for integrating variable generation)," National Renewable Energy Lab.(NREL), Golden, CO (United States), Tech. Rep., 2019.

[26] TAMU, "Electric grid test case repository," [Online] Available at: https://electricgrids.engr.tamu.edu/electric-grid-test-cases/activsg2000.

[27] A. Lokhov, "Load-following with nuclear power plants," *NEA news*, vol. 29, no. 2, pp. 18–20, 2011.

[28] "Gridpath: Advanced Software for Power- System Planning," [Online] Available at: https://www.gridpath.io.

[29] NREL, "Archives: NREL ATB and Standard Scenarios," [Online] Available at: https://atb.nrel.gov/archive, [Accessed: 24 Aug. 2023].

[30] USNRC, "Application Documents for the Nuscale us600 Design," [Online] Available at: https://www.nrc.gov/reactors/new-reactors/smr/licensing-activities/nuscale/documents.html, [Accessed: 24 Aug. 2023].

[31] S. Subedi, M. Blonsky, Y. Son, and B. Mather, "Cost-benefit analysis of grid-supportive loads for fast frequency response," in *2023 IEEE PES Grid Edge Technologies Conference & Exposition (Grid Edge)*. IEEE, 2023, pp. 1–5.

[32] NREL, "NREL-118 system database," [Online] Available at: http://www.nrel.gov/esif/assets/docs/input-files.zip, [Accessed: 10 Nov. 2020].
[33] "Ganymede-user-guide," [Online] Available at: http://docs.oithpc.utdallas.edu, [Accessed: 2 March, 2020].
[34] NEI, "The impact of xcel energy's nuclear fleet on the minnesota economy," [Online] Available at: https://www.xcelenergy.com/staticfiles/xe-responsive/Energy%20Portfolio/Electricity/MN-Economic-Benefits-Study-Xcel-Energy-Nuclear-Fleet.pdf, [Accessed: 1 Feb. 2024].

Jubeyer Rahman (Graduate Student Member, IEEE) received the B.S. degree in electrical and electronic engineering from Bangladesh University of Engineering and Technology in 2012, and the M.S. degree in electrical engineering from the University of Hawaii at Manoa, Honolulu, HI, USA in 2018, and the Ph.D. degree in electrical engineering from the University of Texas at Dallas, Richardson, TX, USA in 2023. He is currently working at GE Digital as an electricity market software engineer. His research interests include multi-timescale power system operation, capacity expansion planning of renewable intensive power grid, integrated energy systems, microgrid control, electricity and energy market, etc.

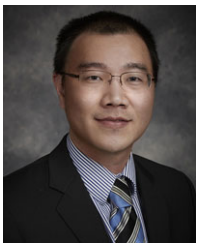

Jie Zhang (Senior Member, IEEE) received the B.S. and M.S. degrees in mechanical engineering from the Huazhong University of Science and Technology, Wuhan, China, in 2006 and 2008, respectively, and the Ph.D. degree in mechanical engineering from Rensselaer Polytechnic Institute, Troy, NY, USA, in 2012. He is currently an Associate Professor with the Department of Mechanical Engineering and (Affiliated) Department of Electrical and Computer Engineering, The University of Texas at Dallas. His research interests include integrated energy systems, renewable energy grid integration, complex networks, machine learning, and multidisciplinary design optimization.